

# Self-Supervised Consistent Quantization for Fully Unsupervised Image Retrieval

Guile Wu\*      Chao Zhang<sup>1</sup>      Stephan Liwicki<sup>1</sup>

<sup>1</sup>Toshiba Europe Limited, Cambridge, UK

guile.wu@outlook.com, {czhang, stephan.liwicki}@crl.toshiba.co.uk

## Abstract

*Unsupervised image retrieval aims to learn an efficient retrieval system without expensive data annotations, but most existing methods rely heavily on handcrafted feature descriptors or pre-trained feature extractors. To minimize human supervision, recent advance proposes deep fully unsupervised image retrieval aiming at training a deep model from scratch to jointly optimize visual features and quantization codes. However, existing approach mainly focuses on instance contrastive learning without considering underlying semantic structure information, resulting in sub-optimal performance. In this work, we propose a novel self-supervised consistent quantization approach to deep fully unsupervised image retrieval, which consists of part consistent quantization and global consistent quantization. In part consistent quantization, we devise part neighbor semantic consistency learning with codeword diversity regularization. This allows to discover underlying neighbor structure information of sub-quantized representations as self-supervision. In global consistent quantization, we employ contrastive learning for both embedding and quantized representations and fuses these representations for consistent contrastive regularization between instances. This can make up for the loss of useful representation information during quantization and regularize consistency between instances. With a unified learning objective of part and global consistent quantization, our approach exploits richer self-supervision cues to facilitate model learning. Extensive experiments on three benchmark datasets show the superiority of our approach over the state-of-the-art methods.*

## 1. Introduction

Image retrieval is a fundamental task in computer vision, aiming to find images that are visually similar to a given query image from a large database. To reduce computational cost and improve storage efficiency, ap-

proximate nearest neighbor search [17] has been widely used, where hashing [4, 38, 47, 50] and product quantization [18, 19, 21, 41] are two most representative directions. Hashing maps real-value embeddings to binary codes for efficient retrieval, while product quantization divides real-value data space into disjoint partitions to quantize embeddings for efficient retrieval. In the past decade, the incredible success of deep learning in computer vision has brought a great breakthrough to deep supervised hashing [3, 26, 50] and deep supervised quantization [2, 21, 49] based image retrieval. Although deep supervised image retrieval methods have shown outstanding performance, the reliance of expensive label annotations of training data hinders their applications in label-limited scenarios.

On the other hand, unsupervised image retrieval is capable of learning an efficient retrieval system without using labeled training data. Traditional unsupervised image retrieval methods [1, 14, 30] utilize handcrafted descriptors to extract embeddings of input images and adopt unsupervised hashing or quantization approaches to efficient retrieval. Recent deep unsupervised image retrieval methods [27, 41, 47] resort to ImageNet [36] pre-trained deep neural networks for feature extraction and incorporate deep hashing or deep quantization techniques into a deep model for optimization. However, these methods either rely on human supervision for devising effective handcrafted feature descriptors or supervised pre-trained ImageNet backbone networks. To minimize human supervision, deep fully unsupervised image retrieval is recently proposed in [18], which aims to train a deep model from scratch to jointly optimize visual features and codes for efficient image retrieval. Despite the self-supervised product quantization approach introduced in [18] has shown promising performance, it only focuses on instance cross quantized contrastive learning without considering underlying semantic structure information, resulting in sub-optimal performance.

In this work, we introduce a novel Self-Supervised Consistent Quantization (SSCQ) approach to deep fully unsupervised image retrieval. We propose to explore richer part and global self-supervision for learning underlying semantic structure information to facilitate model learning. An

\* Work done when G. Wu was an intern at Toshiba Europe Limited.

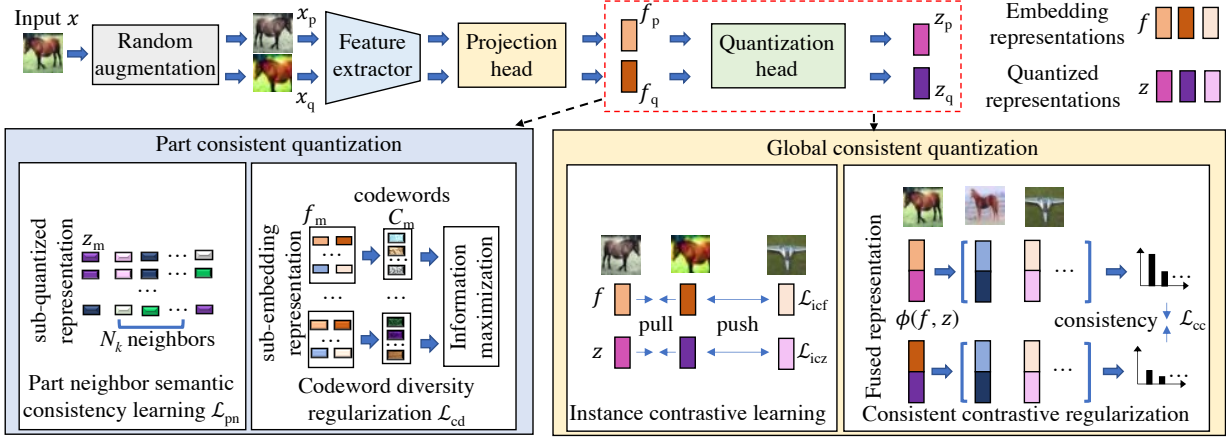


Figure 1. An overview of the proposed Self-Supervised Consistent Quantization (SSCQ) approach to deep fully unsupervised image retrieval. Part consistent quantization discovers part neighbor affinity as self-supervision, while global consistent quantization learns instance affinity as self-supervision, which together are formulated into a unified learning objective for model optimization.

overview of the proposed approach is depicted in Fig. 1. It is known that neighbors in embedding space usually share useful semantic information [15, 44], since the quantization process in product quantization is akin to clustering, the sub-quantized representations should also share underlying neighbor semantic structure information. In light of this, with a contrastive quantization baseline [18], we devise part neighbor semantic consistency learning with codeword diversity regularization [21, 23] to encourage semantic consistency of neighbors of sub-quantized representations. This resolves the limitation of the existing contrastive quantization methods [18, 41] that fail to learn underlying semantic structure information. We term this process *part consistent quantization*. Meanwhile, since it is inevitable that the reconstruction in the quantization process will lose useful information of embedding representations, we apply instance contrastive learning for both embedding and quantized representations to simultaneously optimize visual features and codes so as to make up for the loss. Besides, we fuse the embedding and quantized representations and apply consistent contrastive regularization to regularize consistency between instances. We term this process *global consistent quantization*. Both global and part consistent quantization are formulated into a unified learning objective to explore richer self-supervision for deep fully unsupervised image retrieval. To evaluate the effectiveness of the proposed approach, we conduct extensive experiments on three benchmark datasets, namely CIFAR-10 [24], NUS-WIDE [6] and FLICKR25K [16]. Experimental results show the superiority of our approach over the state-of-the-art methods.

Our **contributions** are: We propose a novel self-supervised consistent quantization approach consists of global consistent quantization and part consistent quantization to deep fully unsupervised image retrieval. In part

consistent quantization, we use part neighbor semantic consistency learning with codeword diversity regularization, which helps to learn underlying neighbor semantic structure information of sub-quantized representations. In global consistent quantization, we employ contrastive learning for both embedding and quantized representations and fuse these representations for consistent contrastive regularization, which helps to make up for the loss of useful representation information during quantization and regularize consistency between instances.

## 2. Related Work

**Unsupervised Image Retrieval.** Most traditional image retrieval methods are originally designed for unsupervised learning scenarios where no labeled training data are used for model learning. The common practice usually consists of two disjoint steps. The first step is to use hand-crafted descriptors, such as GIST [34] and SIFT [32], to extract features of input images, while the second step is to employ binary hashing [4, 37, 43] or product quantization [1, 10, 19] to transform embedding space into Hamming space or a Cartesian product of subspaces for efficient image retrieval. In the past decade, deep learning based methods have dominated the field of image retrieval. Supervised deep hashing [26, 50] or deep product quantization [21, 49] based image retrieval methods have shown notably better performance than the traditional counterparts. However, these supervised methods are limited by the availability of labeled data for model training. To resolve this problem, researchers have resorted to deep unsupervised learning for image retrieval. One of the most popular direction is deep unsupervised hashing [27, 47]. An ImageNet [36] pre-trained deep neural network is usually used as the feature encoder and then hashing layers are inserted

into the model to learn discriminative binary codes using unlabeled data. Despite outstanding performance has been achieved, deep unsupervised hashing relies heavily on the pre-trained feature encoder and can only learn restricted binary codes, limiting its ability for distinguishing visually similar but semantic dissimilar data. Since product quantization is capable of learning continuous representations for efficient image retrieval, deep unsupervised product quantization [18, 41] is recently introduced for unsupervised image retrieval. In [41], soft quantization [49] is combined with contrastive learning [5] and code memory to learn a retrieval system in an unsupervised manner. However, [41] still requires using a pre-trained model as the feature extractor and most layers are not optimized during model training. To minimize human supervision, deep fully unsupervised image retrieval is introduced in [18], which aims to train a deep model from scratch for efficient image retrieval. In [18], a cross-quantized contrastive learning framework is proposed to jointly optimize visual features and codes for unsupervised image retrieval.

Our work belongs to deep unsupervised product quantization and focuses on deep fully unsupervised image retrieval without data label annotation nor supervised pre-trained backbone models. We propose a novel self-supervised consistent quantization approach to discover richer self-supervision to facilitate model optimization. We devise part consistent quantization to discover underlying neighbor semantic structure information and global consistent quantization to learn affinity between instances. This differs from [18] that only uses contrastive learning to optimize cross-quantized representations or [41] that requires a pre-trained model as the feature encoder as well as an additional code memory.

**Self-Supervised Representation Learning.** In recent years, self-supervised/unsupervised representation learning has made great progress. The common practice is devising different pretext tasks, such as predicting image rotation [22] and solving jigsaw puzzles [33], to generate self-supervision information to facilitate unsupervised representation learning. Recently, contrastive learning [5, 12, 42, 45] has become one of the most popular and powerful paradigms for unsupervised representation learning. It usually applies strong random augmentation to each input image to generate positive counterparts and employs a contrastive loss to pull the positives closer and push the negatives apart, where different instances are considered as negatives. In deep fully unsupervised image retrieval, [18] introduces a contrastive quantization framework which shows promising performance compared with conventional unsupervised image retrieval methods even without supervised pre-training. Our approach introduces self-supervised consistent quantization to discover underlying neighbor seman-

tic structure information from sub-quantized representations and to learn affinity between instance so as to facilitate model learning in deep fully unsupervised image retrieval.

### 3. Methodology

**Problem Statement.** In this work, we study deep fully unsupervised image retrieval [18], where no labeled training data nor pre-trained models are available. Given an unlabeled training set  $\mathcal{X}=\{x_i\}_{i=1}^N$  with  $N$  unlabeled samples, our task is to learn a model to encode  $x_i$  into a  $L$ -bit code  $B_i=\{b_i^j\}_{j=1}^L$ , where  $b_i^j\in\{0, 1\}$ , for efficient image retrieval. During inference, the similarity between query and database samples are measured based the learned representations and codes so as to realize efficient retrieval.

#### 3.1. Approach Overview

An overview of the proposed Self-Supervised Consistent Quantization (SSCQ) approach is depicted in Fig. 1. In each training mini-batch  $\{x_i\}_{i=1}^{N_b}$ , we apply strong random data augmentation [5] on each input sample to generate two augmented views, so we have  $2N_b$  augmented samples in each mini-batch. Then, we extract a  $D$ -dimensional embedding representations  $f_i$  of an augmented input  $x_i$  and further quantize  $f_i$  into a  $D$ -dimensional quantized representation  $z_i$ . To construct the model training objective, we employ part and global consistent quantization. In part consistent quantization, we compute a part neighbor semantic consistency learning loss  $\mathcal{L}_{pn}$  for each sub-quantized representation and use entropy maximization  $\mathcal{L}_{cd}$  to regularize the diversity of codewords. Meanwhile, in global consistent quantization, we compute instance contrastive learning loss  $\mathcal{L}_{icf}$  for embedding representations  $\{f_i\}_{i=1}^{2N_b}$  and  $\mathcal{L}_{icz}$  for quantized representations  $\{z_i\}_{i=1}^{2N_b}$  respectively, and compute consistent contrastive regularization  $\mathcal{L}_{cc}$  with fused representations  $\{\phi(f_i, z_i)\}_{i=1}^{2N_b}$ . Therefore, the unified learning objective is formulated as:

$$\mathcal{L} = \mathcal{L}_{icz} + \lambda_{pn}\mathcal{L}_{pn} + \lambda_{cd}\mathcal{L}_{cd} + \mathcal{L}_{icf} + \lambda_{cc}\mathcal{L}_{cc}, \quad (1)$$

where  $\lambda_{pn}$ ,  $\lambda_{cd}$  and  $\lambda_{cc}$  are weighting parameters. In the following section, we drop the subscript  $i$  (e.g., let  $x$  denote an input  $x_i$ ) if the context is clear.

#### 3.2. Self-Supervised Consistent Quantization

**A Baseline with Contrastive Quantization.** We employ a contrastive quantization baseline model [18] for deep fully unsupervised image retrieval. As shown in Fig. 1, with each augmented input sample  $x$ , a feature extractor is used to extract feature of  $x$  and a projection head is employed to map the learned feature into a  $D$ -dimensional embedding representation  $f$ . The feature extractor is constructed with a deep convolutional neural network, while the projection head is a Multi-Layer Perceptron (MLP) where the

first fully connected (FC) layer maps the feature to 512-dimension following a ReLU layer and the second FC layer outputs a  $D$ -dimensional  $f$ . Then, a quantization head is used to reconstruct  $f$  into a  $D$ -dimensional quantized representation  $z$ . Suppose there are  $M$  codebooks  $\{C_m\}_{m=1}^M$  in the quantization head and each codebook is composed of  $K$  codewords  $C_m = \{c_{m,k}\}_{k=1}^K$ , where  $c_{m,k} \in \mathbb{R}^{M/D}$ . Following product quantization [19, 49],  $f$  is divided into  $M$  disjoint sub-embedding representation  $f_m \in \mathbb{R}^{M/D}$  and the codewords in the  $m$ -th codebook attempt to reconstruct the sub-embedding representation  $f_{i,m}$ . Therefore, the embedding space is divided into a Cartesian product of  $M$  subspaces  $\{C_1 \times C_2 \times \dots \times C_M\}$ , and codewords in the  $m$ -th codebook are considered as distinct clustered centroids of the  $m$ -th sub-embedding representations of all samples. This allows to cluster visually similar sub-embedding representations into the same codeword for efficient similarity measurement. To train the feature extractor, the projection head and the quantization head in an end-to-end manner, soft quantization [49] is employed for training, so the sub-quantized representation  $z_m$  is defined as:

$$z_m = \sum_{k=1}^K \frac{\exp(d(f_m, c_{m,k})/\tau_{sq})}{\sum_{j=1}^K \exp(d(f_m, c_{m,j})/\tau_{sq})} c_{m,k}, \quad (2)$$

where  $d(f_m, c_{m,k}) = -\|f_m - c_{m,k}\|_2^2$  is the squared Euclidean distance, and  $\tau_{sq}$  is a temperature parameter,  $z$  is the concatenation of  $z_m$ .

To optimize the model, an instance contrastive learning loss  $\mathcal{L}_{icz}$  [5] is computed to pull  $z$  closer to its positive (the reconstructed representation of augmented counterparts from the same input) and push its negatives apart (the reconstructed representations of other augmented samples of different inputs), as:

$$\mathcal{L}_{icz} = -\log \frac{\exp(s(z, z^+)/\tau_{ic})}{\sum_{j=1}^{2N_b} \mathbb{1}_{[z_j \neq z]} \exp(s(z, z_j)/\tau_{ic})}, \quad (3)$$

where  $z$  and  $z^+$  are positive pairs of the same input,  $s(z, z^+) = z^T z^+ / (\|z\| \|z^+\|)$  is cosine similarity between  $z$  and  $z^+$ ,  $\mathbb{1}_{[z_j \neq z]}$  denotes an indicator function, and  $\tau_{ic}$  is a temperature parameter.

With the baseline model, [18] reformulates a cross quantized contrastive learning loss to learn the correlation between the embedding representation  $f$  and the quantized representation  $z$ . However, it only considers instance contrastive learning and largely ignores the underlying semantic structure information. To resolve this problem, we propose to use part and global consistent quantization to explore richer self-supervision cues for model optimization.

**Part Consistent Quantization.** The quantization process in the quantization head is akin to clustering by learning

distinct codewords as cluster centroids but with learnable parameters for end-to-end model training. Thus, each sub-quantized representation  $z_m$  inherently encodes part neighbor semantic structure information, which can be exploited as auxiliary self-supervision cues to facilitate model learning. In light of this, we use a part neighbor semantic consistency learning loss  $\mathcal{L}_{pn}$  to pull each sub-quantized representation  $z_m$  closer to its similar sub-quantized representations and push  $z_m$  away from dissimilar ones, as:

$$\mathcal{L}_{pn} = -\frac{1}{M} \sum_{m=1}^M \log \frac{\sum_{n=1}^{N_k} \exp(s(z_m, z_{m,n}^-)/\tau_{pn})}{\sum_{j=1}^{2N_b-2} \exp(s(z_m, z_{m,j}^-)/\tau_{pn})}, \quad (4)$$

where  $\tau_{pn}$  is a temperature parameter, and  $\{z_{m,n}^-\}_{n=1}^{N_k}$  are the top  $N_k$  part neighbors of  $z_m$  which are obtained by computing the similarity between  $z_m$  and its negative sub-quantized representations  $z_m^-$ . Here,  $\mathcal{L}_{pn}$  differs from existing unsupervised neighbor discovery methods [15, 44, 48] in that  $\mathcal{L}_{pn}$  mines neighbor affinity between sub-quantized representations  $z_m$  and its negatives  $z_{m,n}^-$  to facilitate quantization, instead of progressively exploring anchored neighbors [15] or maintaining a patch/tracklet memory bank [44, 48].

Besides, to encourage diverse codeword distribution, we compute the similarity between sub-embedding representations and codewords in each codebook and encourage the mean probability distribution to be diverse, as:

$$\mathcal{L}_{cd} = \frac{1}{M} \sum_{m=1}^M \sum_{k=1}^K \hat{p}_{m,k} \cdot \log(\hat{p}_{m,k}), \quad (5)$$

where  $\hat{p}_{m,k} = \frac{1}{2N_b} \sum_i \frac{\exp(s(f_{i,m}, c_{m,k}))}{\sum_{t=1}^K \exp(s(f_{i,m}, c_{m,t}))}$  is the mean output probability over all samples in a mini-batch. Note that similar codeword diversity regularization has been used in previous quantization method [21], but here  $\mathcal{L}_{cd}$  in our approach is an auxiliary term based on entropy maximization [23, 28] for unsupervised part consistent quantization and is not directly computed using soft quantization code.

**Global Consistent Quantization.** Previous contrastive quantization based methods [18, 41] mainly use contrastive learning for quantized or cross-quantized representations. However, it is inevitable that quantized representations lose some useful embedding representation information during reconstruction in the quantization process. This issue potentially hinders model optimization when the feature extractor is not pre-trained and not fixed in an end-to-end trainable framework. To address this issue, as shown in Fig. 1, in addition to  $\mathcal{L}_{icz}$ , we also compute an instance contrastive learning loss  $\mathcal{L}_{icf}$  for the embedding representations  $f$ , as:

$$\mathcal{L}_{icf} = -\log \frac{\exp(s(f, f^+)/\tau_{ic})}{\sum_{j=1}^{2N_b} \mathbb{1}_{[f_j \neq f]} \exp(s(f, f_j)/\tau_{ic})}. \quad (6)$$



With Eqs.(3) and (6), we can simultaneously optimize the reconstructed quantized representations and the original embedding representations to jointly learn visual features and codes.

Furthermore, recent advance in unsupervised representation learning [25, 42] indicates that exploring the affinity between positive and negative instances in contrastive learning is beneficial to model optimization for better generalization. To further facilitate unsupervised quantization, we apply a consistent contrastive regularization [42]  $\mathcal{L}_{cc}$  to the global consistent quantization. Directly applying  $\mathcal{L}_{cc}$  on model outputted quantized representations may not fully explore global semantic information. Thus, we first fuse  $f$  and  $z$  in order to learn the potential correlation between embedding and quantized representations, i.e., generate the fused representation  $\Phi(f, z)$  where  $\Phi(\cdot, \cdot)$  is the fusion operation (e.g., concatenation or sum fusion). Then, we compute the similarity  $Q(j)$  between  $\Phi(f, z)$  and its negatives  $\{\Phi(f^-, z^-)_j\}_{j=1}^{2N_b-2}$  and the similarity  $P(j)$  between  $\Phi(f^+, z^+)$  and the same negatives, as:

$$Q(l) = \frac{\exp(s(\Phi(f, z), \Phi(f^-, z^-)_l)/\tau_{cc})}{\sum_{j=1}^{2N_b-2} \exp(s(\Phi(f, z), \Phi(f^-, z^-)_j)/\tau_{cc})},$$

$$P(l) = \frac{\exp(s(\Phi(f^+, z^+), \Phi(f^-, z^-)_l)/\tau_{cc})}{\sum_{j=1}^{2N_b-2} \exp(s(\Phi(f^+, z^+), \Phi(f^-, z^-)_j)/\tau_{cc})}, \quad (7)$$

where  $\tau_{cc}$  is a temperature parameter. Since unlabeled samples in a training set can usually be categorized into multiple semantical categories where each category contains multiple samples, the similarity between an instance and its negatives potentially encodes the neighbor semantic structure information. By regularizing the consistency of similarity probability distribution between an instance and its positive, we can encourage the model to output consistent predictions between different augmented instances from the same input. Thus, using the symmetric Kullback-Leibler Divergence  $D_{KL}$ ,  $\mathcal{L}_{cc}$  is defined as:

$$\mathcal{L}_{cc} = \frac{1}{2}(D_{KL}(P\|Q) + D_{KL}(Q\|P)). \quad (8)$$

Note that the fused representation  $\Phi(f, z)$  is built on the instance contrastive learning of both  $f$  and  $z$ , so if only  $z$  is optimized with contrastive learning, then  $\Phi(f, z) = z$ . Alternatively, we can compute cross consistent contrastive regularization in Eqs.(7) and (8) for embedding and quantized representations to encourage consistent predictions between them.

**Summary.** We summarize the training process of the proposed Self-Supervised Consistent Quantization in Algorithm 1. In training, a unified learning objective (Eq.(1)) based on part and global consistent quantization is formu-

---

**Algorithm 1** Self-Supervised Consistent Quantization.

---

**Input:** A baseline model, unlabeled training data  $\mathcal{X}$

- 1: **for** sampled mini-batch  $\{x_i\}_{i=1}^{N_b}$  **do**
- 2:   Generate two augmented samples for each  $x$
- 3:   Extract embedding representation  $f$  of all samples
- 4:   Extract quantized representation  $z$  of all samples
- 5:   Compute  $\mathcal{L}_{icz}$  for  $z$  (Eq.(3))
- 6:   /\* Part consistent quantization \*/
- 7:   Compute  $\mathcal{L}_{pn}$  for  $z_m$  (Eq.(4))
- 8:   Compute  $\mathcal{L}_{cd}$  for  $f_m$  and  $c_{m,k}$  (Eq.(5))
- 9:   /\* Global consistent quantization \*/
- 10:   Compute  $\mathcal{L}_{icf}$  for  $f$  (Eq.(6))
- 11:   Compute  $\mathcal{L}_{cc}$  for fused  $\phi(f, z)$  (Eq.(8))
- 12:   /\* Unified learning objective \*/
- 13:   Optimize the model with  $\mathcal{L}$  (Eq.(1))
- 14: **end for**

**Output:** A trained model for image retrieval.

---

lated for model learning. In inference, following the previous work [18, 41], we use hard quantization to generate the  $(M \cdot \log_2 K)$ -bits code for each sample in the database by finding the most similar codeword  $\{c_{m,k}\}_{k=1}^K$  in each codebook  $\{C_m\}_{m=1}^M$  for each sub-embedding representation. Then, we use asymmetric distance [19] to measure the distance between each query sample and database samples. Specifically, given a query image, we extract its embedding representation and divide it into  $M$  sub-embedding representations. Next, we compute the Euclidean distance between each sub-embedding representation and all codewords in all codebooks to set up a query-specific look-up table. Finally, we can approximately calculate the distance between the query sample and each database sample by using the code to get the sub-vector distance from the query-specific look-up table and summing up.

## 4. Experiments

### 4.1. Dataset and Evaluation Protocol

**Datasets.** To evaluate the proposed self-supervised consistent quantization approach for fully unsupervised image retrieval, we conduct extensive experiments on three datasets, namely CIFAR-10 [24], NUS-WIDE [6] and FLICKR25K [16]. **CIFAR-10** consists of 60,000 images of 10 class, where each class has 5,000 images for training and 1,000 images for testing. We use 1,000 images per class as the query set, while the remaining images are used as the training set and the retrieval database. **NUS-WIDE** is a multi-label large-scale dataset with around 270,000 images of 81 categories. We select images of the 21 most frequent categories for evaluation, where 100 images per categories are selected to form 21,000 images as the query set while the remaining images form the training set and the retrieval

database. **FLICKR25K** is a relatively small dataset with 25,000 images of 24 categories. We randomly select 2,000 images as the query set while the remaining images are used as the training set and the retrieval database.

**Evaluation Metrics.** Following [18, 27, 38, 41], we mainly employ mean Average Precision (mAP, %) as the evaluation metric. We use mAP@1000 for CIFAR-10 and mAP@5000 for NUS-WIDE and FLICKR25K, and report image retrieval results with  $\{16, 32, 64\}$  bits codes. Besides, we also report Precision-Recall curves (PR) and Precision curves with top-1000 returned samples ( $P@1000$ ) at 32 bits codes. On the multi-label NUS-WIDE and FLICKR25K, if a query image and a database image share at least one label, then they are defined as the true match [18, 27].

**Implementation Details.** We implement our approach with Python and PyTorch. Following [18], we use the modified ResNet-18 [13, 18] as the backbone (feature extractor) for CIFAR-10 where the first convolutional layer is modified with small kernel size and stride to adapt to the small  $32 \times 32$  input image size, and use standard ResNet-50 [13] as the backbone for NUS-WIDE and FLICKR25K. We use strong random augmentation [5], including random cropping, horizontal flipping, color jitter, gray scaling and Gaussian blur, to generate augmented samples. The number of codewords in each codebook is fixed to  $K=2^4$ , the dimension of each codeword is fixed to  $D/M=16$  and the number of codebook is varying as  $M=\{4, 8, 16\}$ , so we can generate  $\{M \cdot \log_2 K\}=\{16, 32, 64\}$  bits codes for image retrieval. We use Adam [20] as the optimizer with the initial learning rate of  $5e-4$  for CIFAR-10 and  $2e-4$  for NUS-WIDE and FLICKR25K, and set the weight decay of  $1e-5$ . We warm up the learning rate with 10 epochs and decay it with the cosine decay schedule [31] without restart. On CIFAR-10, we set the batch size  $N_B=256$  with the original input image size of  $32 \times 32$ , while on NUS-WIDE and FLICKR25K,  $N_B=128$  with the input image size of  $224 \times 224$ . In part consistent quantization, we set  $\lambda_{pn}=0.1$ ,  $\lambda_{cd}=0.2$ ,  $N_k=20$ ,  $\tau_{pn}=0.5$ . In global consistent quantization, we set  $\tau_{sq}=0.2$  and  $\tau_{ic}=0.5$  following [18], and use  $\lambda_{cc}=0.4$  and  $\tau_{cc}=0.2$ . In fully unsupervised image retrieval, we train our model from scratch without using ImageNet [36] pre-trained weights. Note that despite our approach is devised for deep fully unsupervised image retrieval, it is compatible with the deep pre-trained unsupervised setting, so we also report SSCQ-p that employs an ImageNet pre-trained VGG16 model as the backbone.

## 4.2. Comparison with the State-of-the-Arts

We compared our SSCQ and SSCQ-p with three types of classic and state-of-the-art unsupervised image retrieval methods, including (1) shallow methods with input features extracted from an ImageNet pre-trained VGG16

Type	Method	16 bits	32 bits	64 bits
Shallow + pre-trained	LSH [4]	13.2	15.8	16.7
	SpectralH [43]	27.2	28.5	30.0
	PQ [19]	23.7	25.9	27.2
	ITQ [11]	30.5	32.5	34.9
	OPQ [10]	29.7	31.4	32.3
Deep pre-trained unsupervised	DeepBit [29]	22.0	24.9	27.7
	SAH [9]	41.8	45.6	47.4
	GreedyHash [40]	44.8	47.3	50.1
	SSDH [46]	36.2	40.2	44.0
	TBH [38]	53.2	57.3	57.8
	CIBHash [35]	59.4	63.7	65.2
	Bi-half [27]	56.1	57.6	59.5
	MeCoQ [41]	68.2	69.7	71.1
Deep fully unsupervised	SSCQ-p (ours)	<b>76.1</b>	<b>76.8</b>	<b>78.1</b>
	SGH [7]	43.5	43.7	43.3
	HashGAN [8]	44.7	46.3	48.1
	BinGAN [51]	47.6	51.2	52.0
	SPQ [18]	76.8	79.3	81.2
	SSCQ (ours)	<b>78.3</b>	<b>81.3</b>	<b>82.9</b>

Table 1. Comparison with the classic and state-of-the-art unsupervised methods on CIFAR-10 in terms of mAP (%). Some results are cited from [18, 41].

Type	Method	16 bits	32 bits	64 bits
Shallow + pre-trained	LSH [4]	38.5	41.4	43.9
	SpectralH <sup>†</sup> [43]	48.9	53.0	62.7
	PQ [19]	65.4	67.4	68.6
	ITQ <sup>†</sup> [11]	68.0	70.9	72.8
	OPQ [10]	65.7	68.4	69.1
Deep pre-trained unsupervised	DeepBit [29]	39.2	40.3	42.9
	GreedyHash [40]	63.3	69.1	73.1
	SSDH [46]	58.0	59.3	61.0
	CIBHash <sup>†</sup> [35]	79.5	81.2	81.7
	Bi-half [27]	76.9	78.3	79.9
	MeCoQ <sup>†</sup> [41]	77.2	81.5	82.3
	SSCQ-p (ours)	<b>80.3</b>	<b>81.9</b>	<b>82.6</b>
Deep fully unsupervised	SGH [7]	59.3	59.0	60.7
	HashGAN [8]	68.4	70.6	71.7
	BinGAN [51]	65.4	70.9	71.3
	SPQ <sup>†</sup> [18]	75.7	79.4	80.2
	SSCQ (ours)	<b>78.7</b>	<b>79.9</b>	<b>80.8</b>

Table 2. Comparison with the classic and state-of-the-art unsupervised methods on NUS-WIDE in terms of mAP (%). Some results are cited from [41]. <sup>†</sup> Reproduced results.

model [39], such as SpectralH [43] and ITQ [11]; (2) deep pre-trained unsupervised methods which use an ImageNet pre-trained VGG16 model [39] as the backbone and optimize certain layers to generate codes in an unsupervised learning manner, such as Bi-half [27] and MeCoQ [41]; (3) deep fully unsupervised methods which train a model from scratch and jointly optimize visual features and codes in an unsupervised learning manner, such as SPQ [18].

On CIFAR-10, as shown in Table 1, our SSCQ approach achieves the best performance on all bits. SSCQ improves the second-best SPQ [18] by 1.5%, 2.0% and 1.7% on 16

Type	Method	16 bits	32 bits	64 bits
Shallow + pre-trained	LSH [4]	58.8	60.4	64.2
	SpectralH [43]	59.2	60.6	63.2
	ITQ [11]	68.4	69.5	70.3
Deep pre-trained unsupervised	GreedyHash [40]	70.5	72.3	75.1
	SSDH [46]	78.7	79.4	79.5
	CIBHash [35]	77.0	78.5	79.8
	Bi-half [27]	81.1	82.4	<b>82.9</b>
	MeCoQ [41]	80.4	81.7	81.7
	SSCQ-p (ours)	<b>81.9</b>	<b>82.6</b>	82.8
Deep fully unsupervised	SPQ [18]	71.8	74.0	74.5
	SSCQ (ours)	<b>73.8</b>	<b>75.9</b>	<b>76.7</b>

Table 3. Comparison with the classic and state-of-the-art unsupervised methods on FLICKR25K in terms of mAP (%).

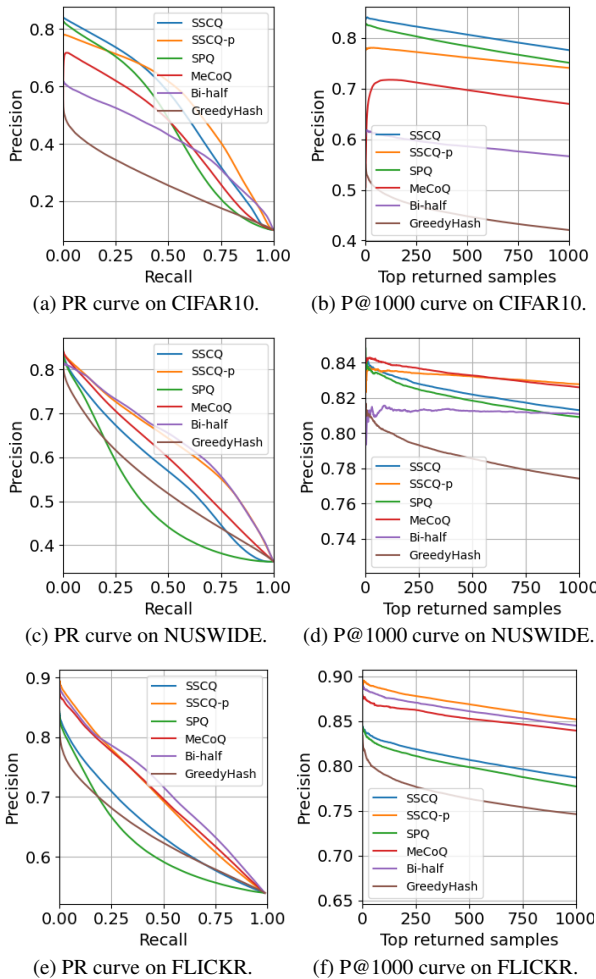


Figure 2. PR curves and P@1000 curves on CIFAR-10, NUS-WIDE and FLICKR25K (32 bits).

bits, 32 bits and 64 bits, respectively. Besides, with a pre-trained backbone model, our SSCQ-p approach also outperforms the state-of-the-art deep pre-trained unsupervised methods, such as Bi-half [27] and MeCoQ [41], by a distinct

Component					mAP (%)		
$\mathcal{L}_{icz}$	$\mathcal{L}_{pn}$	$\mathcal{L}_{cd}$	$\mathcal{L}_{icf}$	$\mathcal{L}_{cc}$	16 bits	32 bits	64 bits
✓	-	-	-	-	74.2	77.6	78.5
✓	✓	-	-	-	77.3	79.2	80.8
✓	✓	✓	-	-	77.9	80.6	81.9
✓	-	-	✓	-	76.5	80.0	80.8
✓	-	-	✓	✓	76.8	80.2	81.4
✓	✓	✓	✓	✓	<b>78.3</b>	<b>81.3</b>	<b>82.9</b>

Table 4. Component effectiveness evaluation on CIFAR-10.

margin. On the large-scale multi-label NUS-WIDE dataset, as shown in Table 2, our SSCQ outperforms the state-of-the-art deep fully unsupervised SPQ by 3.0%, 0.5% and 0.6% on 16 bits, 32 bits and 64 bits respectively. And our SSCQ-p achieves 80.3%, 81.9% and 82.6% on 16 bits, 32 bits and 64 bits respectively, which are competitive against the state-of-the-art deep pre-trained unsupervised MeCoQ. On the relatively small-scale FLICKR25K dataset, as shown in Table 3, our SSCQ improves the state-of-the-art deep fully unsupervised SPQ approximately 2% on all bits, while our SSCQ-p achieves 81.9%, 82.6% and 82.8% on 16 bits, 32 bits and 64 bits respectively, which are still competitive against the state-of-the-art deep pre-trained unsupervised MeCoQ and Bi-half. In addition, since NUS-WIDE and FLICKR25K are composed of natural images which are close to those from ImageNet, we can observe that SSCQ-p performs better than SSCQ, but SSCQ still yields competitive performance even though no pre-trained model is used. This shows that our approach can accommodate to different scenarios and achieve compelling results. Overall, the superior performance of our SSCQ and SSCQ-p can be attributed to exploring richer self-supervision to facilitate the joint optimization of visual features and codes.

Besides, in Fig. 2, we report PR curves and P@1000 curves. It can be observed that our SSCQ (blue curves) consistently outperforms SPQ (green curves) under the fully unsupervised setting, while our SSCQ-p (orange curves) performs competitively against the state-of-the-art pre-trained unsupervised methods. This further shows that our approach is capable of learning effective representations and codes for image retrieval at different required recall rates and numbers of top returned samples.

### 4.3. Ablation Study

In Table 4, we present component effectiveness evaluation of the proposed SSCQ on CIFAR-10. We can observe that: (1) While the baseline model ( $\mathcal{L}_{icz}$ ) achieves 74.2% on 16 bits, 77.6% on 32 bits and 78.5% on 64 bits, the part consistent quantization ( $\mathcal{L}_{icz} + \mathcal{L}_{pn} + \mathcal{L}_{cd}$ ) improves the baseline by 77.9% on 16 bits, 80.6% on 32 bits and 81.9% on 64 bits, respectively. This shows that discovering part neighbor semantic structure information as self-

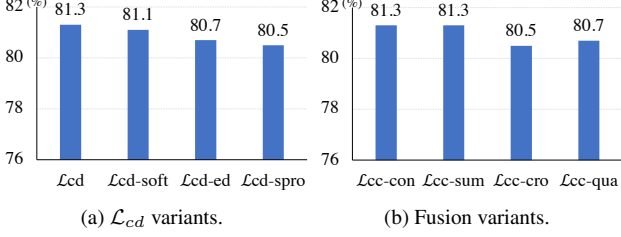


Figure 3. Evaluating (a) codeword diversity regularization variants and (b) representation fusion variants on CIFAR-10 (32 bits).

supervision can improve contrastive quantization. (2) The global consistent quantization ( $\mathcal{L}_{icz} + \mathcal{L}_{icf} + \mathcal{L}_{cc}$ ) also significantly improves the baseline, achieving 76.8% on 16 bits, 80.2% on 32 bits and 81.4% on 64 bits, respectively. This shows the effectiveness of learning the affinity between instances as richer self-supervision for contrastive quantization. (3) SSCQ with the unified learning objective ( $\mathcal{L}_{icz} + \mathcal{L}_{icf} + \mathcal{L}_{cc} + \mathcal{L}_{pn} + \mathcal{L}_{cd}$ ) of global and part consistent quantization yields the best performance, namely 78.3% on 16 bits, 81.3% on 32 bits and 82.9% on 64 bits, which improves the baseline by 4.1% on 16 bits, 3.7% on 32 bits, 4.4% on 64 bits, respectively. These results validate that exploring richer part and global self-supervision in contrastive quantization can facilitate model optimization to obtain better performance.

#### 4.4. Further Analysis and Discussion

**Codeword Diversity Regularization Variants.** As shown in Fig. 3a, we test SSCQ with different codeword distribution regularization strategies, where  $\mathcal{L}_{cd-soft}$  and  $\mathcal{L}_{cd-ed}$  denote soft quantization based or squared Euclidean distance based probability to compute the mean output probability in Eq.(5), and  $\mathcal{L}_{cd-spro}$  denotes using squared probability as [21] in Eq.(5). Overall, SSCQ with entropy maximization based codeword diversity regularization achieves encouraging result.

**Representation Fusion Variants.** In Fig. 3b, we report the performance of SSCQ with different embedding and quantized representations fusion strategies, including concatenation fusion, sum fusion, cross consistent contrastive regularization, as well as directly computing  $\mathcal{L}_{cc}$  with quantized representations. We can observe that SSCQ with  $\mathcal{L}_{cc-con}$  and  $\mathcal{L}_{cc-sum}$  yield compelling results, while SSCQ with  $\mathcal{L}_{cc-cro}$  and  $\mathcal{L}_{cc-qua}$  as [42] achieve slightly worse results.

**Temperature Parameter Sensitivity.** In Fig. 4, we report the performance of our SSCQ with the temperature parameters ( $\tau_{ic}$ ,  $\tau_{sq}$ ,  $\tau_{cc}$  and  $\tau_{pn}$ ) ranging from different values. It can be seen that with different values of  $\tau_{cc}$ ,  $\tau_{pn}$  and  $\tau_{sq}$ , SSCQ still performs competitively and the reasonable range is at around 0.2 for  $\tau_{cc}$ , [0.2, 0.5] for  $\tau_{pn}$  and  $\tau_{sq}$ . As for  $\tau_{ic}$ , it is a basic component of contrastive quantization, so

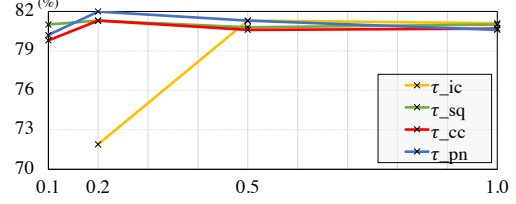


Figure 4. Evaluating temperature parameter sensitivity on CIFAR-10 (32 bits).

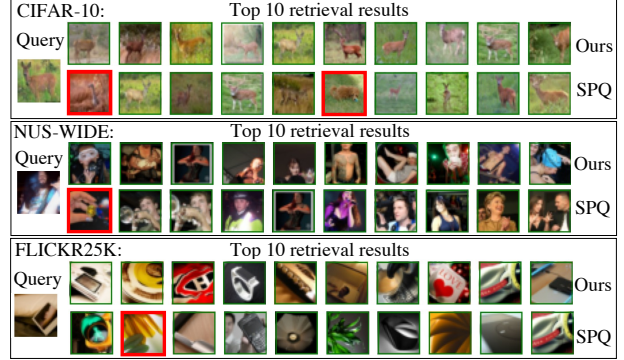


Figure 5. Retrieval results of our approach and SPQ on CIFAR-10, NUS-WIDE and FLICKR25K (32 bits). False retrieval results are in red bounding boxes.

it is more sensitive and yields competitive result at around [0.5, 1.0].

**Qualitative Retrieval Results.** In Fig. 5, we visualize some retrieval results returned by our SSCQ and SPQ [18] respectively. We can see that both SSCQ and SPQ can retrieve visually similar images from the database, but SSCQ tends to explore more discriminative information resulting in more relevant retrieval results. This mainly attributed to discovering richer self-supervision for model learning in SSCQ.

## 5. Conclusion

In this work, we propose a novel Self-Supervised Consistent Quantization (SSCQ) approach to deep fully unsupervised image retrieval. To discover underlying semantic structure information as self-supervision, we devise *part consistent quantization* using part neighbor semantic consistency learning with codeword regularization and *global consistent quantization* using instance contrastive learning with consistent contrastive regularization. We formulate the part and global consistent quantization into a unified learning objective to facilitate model learning. Extensive experiments on three benchmark datasets show the superior performance of our approach over the state-of-the-art methods. In future work, we aim to explore richer self-supervision information to facilitate the joint learning of visual features and codes for more efficient image retrieval.



## References

- [1] Artem Babenko and Victor Lempitsky. Additive quantization for extreme vector compression. In *Proceedings of the IEEE Conference on Computer Vision and Pattern Recognition*, pages 931–938, 2014. 1, 2
- [2] Yue Cao, Mingsheng Long, Jianmin Wang, Han Zhu, and Qingfu Wen. Deep quantization network for efficient image retrieval. In *Proceedings of the AAAI Conference on Artificial Intelligence*, pages 3457–3463, 2016. 1
- [3] Zhangjie Cao, Mingsheng Long, Jianmin Wang, and Philip S Yu. Hashnet: Deep learning to hash by continuation. In *Proceedings of the IEEE International Conference on Computer Vision*, pages 5608–5617, 2017. 1
- [4] Moses S Charikar. Similarity estimation techniques from rounding algorithms. In *Proceedings of the thirty-fourth annual ACM symposium on Theory of computing*, pages 380–388, 2002. 1, 2, 6, 7
- [5] Ting Chen, Simon Kornblith, Mohammad Norouzi, and Geoffrey Hinton. A simple framework for contrastive learning of visual representations. In *International Conference on Machine Learning*, pages 1597–1607. PMLR, 2020. 3, 4, 6
- [6] Tat-Seng Chua, Jinhui Tang, Richang Hong, Haojie Li, Zhiping Luo, and Yantao Zheng. Nus-wide: a real-world web image database from national university of singapore. In *Proceedings of the ACM international conference on image and video retrieval*, pages 1–9, 2009. 2, 5
- [7] Bo Dai, Ruiqi Guo, Sanjiv Kumar, Niao He, and Le Song. Stochastic generative hashing. In *International Conference on Machine Learning*, pages 913–922. PMLR, 2017. 6
- [8] Kamran Ghasedi Dizaji, Feng Zheng, Najmeh Sadoughi, Yanhua Yang, Cheng Deng, and Heng Huang. Unsupervised deep generative adversarial hashing network. In *Proceedings of the IEEE Conference on Computer Vision and Pattern Recognition*, pages 3664–3673, 2018. 6
- [9] Thanh-Toan Do, Dang-Khoa Le Tan, Trung T Pham, and Ngai-Man Cheung. Simultaneous feature aggregating and hashing for large-scale image search. In *Proceedings of the IEEE Conference on Computer Vision and Pattern Recognition*, pages 6618–6627, 2017. 6
- [10] Tiezheng Ge, Kaiming He, Qifa Ke, and Jian Sun. Optimized product quantization for approximate nearest neighbor search. In *Proceedings of the IEEE Conference on Computer Vision and Pattern Recognition*, pages 2946–2953, 2013. 2, 6
- [11] Yunchao Gong, Svetlana Lazebnik, Albert Gordo, and Florent Perronnin. Iterative quantization: A procrustean approach to learning binary codes for large-scale image retrieval. *IEEE Transactions on Pattern Analysis and Machine Intelligence*, 35(12):2916–2929, 2012. 6, 7
- [12] Kaiming He, Haoqi Fan, Yuxin Wu, Saining Xie, and Ross Girshick. Momentum contrast for unsupervised visual representation learning. In *Proceedings of the IEEE/CVF Conference on Computer Vision and Pattern Recognition*, pages 9729–9738, 2020. 3
- [13] Kaiming He, Xiangyu Zhang, Shaoqing Ren, and Jian Sun. Deep residual learning for image recognition. In *Proceedings of the IEEE Conference on Computer Vision and Pattern Recognition*, pages 770–778, 2016. 6
- [14] Jae-Pil Heo, Youngwoon Lee, Junfeng He, Shih-Fu Chang, and Sung-Eui Yoon. Spherical hashing. In *2012 IEEE Conference on Computer Vision and Pattern Recognition*, pages 2957–2964. IEEE, 2012. 1
- [15] Jiabo Huang, Qi Dong, Shaogang Gong, and Xiatian Zhu. Unsupervised deep learning by neighbourhood discovery. In *International Conference on Machine Learning*, pages 2849–2858. PMLR, 2019. 2, 4
- [16] Mark J Huiskes and Michael S Lew. The mir flickr retrieval evaluation. In *Proceedings of the 1st ACM international Conference on Multimedia Information Retrieval*, pages 39–43, 2008. 2, 5
- [17] Piotr Indyk and Rajeev Motwani. Approximate nearest neighbors: towards removing the curse of dimensionality. In *Proceedings of the thirtieth annual ACM symposium on Theory of computing*, pages 604–613, 1998. 1
- [18] Young Kyun Jang and Nam Ik Cho. Self-supervised product quantization for deep unsupervised image retrieval. In *Proceedings of the IEEE/CVF International Conference on Computer Vision*, pages 12085–12094, 2021. 1, 2, 3, 4, 5, 6, 7, 8
- [19] Herve Jegou, Matthijs Douze, and Cordelia Schmid. Product quantization for nearest neighbor search. *IEEE Transactions on Pattern Analysis and Machine Intelligence*, 33(1):117–128, 2010. 1, 2, 4, 5, 6
- [20] Diederik P Kingma and Jimmy Ba. Adam: A method for stochastic optimization. *arXiv preprint arXiv:1412.6980*, 2014. 6
- [21] Benjamin Klein and Lior Wolf. End-to-end supervised product quantization for image search and retrieval. In *Proceedings of the IEEE/CVF Conference on Computer Vision and Pattern Recognition*, pages 5041–5050, 2019. 1, 2, 4, 8
- [22] Nikos Komodakis and Spyros Gidaris. Unsupervised representation learning by predicting image rotations. In *International Conference on Learning Representations (ICLR)*, 2018. 3
- [23] Andreas Krause, Pietro Perona, and Ryan Gomes. Discriminative clustering by regularized information maximization. *Advances in Neural Information Processing Systems*, 23, 2010. 2, 4
- [24] Alex Krizhevsky and Geoffrey Hinton. Learning multiple layers of features from tiny images. Technical report, 2009. 2, 5
- [25] Junnan Li, Pan Zhou, Caiming Xiong, and Steven Hoi. Prototypical contrastive learning of unsupervised representations. In *International Conference on Learning Representations*, 2021. 5
- [26] Qi Li, Zhenan Sun, Ran He, and Tieniu Tan. Deep supervised discrete hashing. *Advances in Neural Information Processing Systems*, 30, 2017. 1, 2
- [27] Yunqiang Li and Jan van Gemert. Deep unsupervised image hashing by maximizing bit entropy. In *Proceedings of the AAAI Conference on Artificial Intelligence*, volume 35, pages 2002–2010, 2021. 1, 2, 6, 7

- [28] Jian Liang, Dapeng Hu, and Jiashi Feng. Do we really need to access the source data? source hypothesis transfer for unsupervised domain adaptation. In *International Conference on Machine Learning*, pages 6028–6039. PMLR, 2020. 4
- [29] Kevin Lin, Jiwen Lu, Chu-Song Chen, and Jie Zhou. Learning compact binary descriptors with unsupervised deep neural networks. In *Proceedings of the IEEE Conference on Computer Vision and Pattern Recognition*, pages 1183–1192, 2016. 6
- [30] Wei Liu, Cun Mu, Sanjiv Kumar, and Shih-Fu Chang. Discrete graph hashing. *Advances in Neural Information Processing Systems*, 27, 2014. 1
- [31] Ilya Loshchilov and Frank Hutter. Sgdr: Stochastic gradient descent with warm restarts. *arXiv preprint arXiv:1608.03983*, 2016. 6
- [32] David G Lowe. Distinctive image features from scale-invariant keypoints. *International Journal of Computer Vision*, 60(2):91–110, 2004. 2
- [33] Mehdi Noroozi and Paolo Favaro. Unsupervised learning of visual representations by solving jigsaw puzzles. In *European Conference on Computer Vision*, pages 69–84. Springer, 2016. 3
- [34] Aude Oliva and Antonio Torralba. Modeling the shape of the scene: A holistic representation of the spatial envelope. *International Journal of Computer Vision*, 42(3):145–175, 2001. 2
- [35] Zexuan Qiu, Qinliang Su, Zijing Ou, Jianxing Yu, and Changyou Chen. Unsupervised hashing with contrastive information bottleneck. In *Proceedings of the Thirtieth International Joint Conference on Artificial Intelligence*, 2021. 6, 7
- [36] Olga Russakovsky, Jia Deng, Hao Su, Jonathan Krause, Sanjeev Satheesh, Sean Ma, Zhiheng Huang, Andrej Karpathy, Aditya Khosla, Michael Bernstein, et al. Imagenet large scale visual recognition challenge. *International Journal of Computer Vision*, 115(3):211–252, 2015. 1, 2, 6
- [37] Ruslan Salakhutdinov and Geoffrey Hinton. Semantic hashing. *International Journal of Approximate Reasoning*, 50(7):969–978, 2009. 2
- [38] Yuming Shen, Jie Qin, Jiabin Chen, Mengyang Yu, Li Liu, Fan Zhu, Fumin Shen, and Ling Shao. Auto-encoding twin-bottleneck hashing. In *Proceedings of the IEEE/CVF Conference on Computer Vision and Pattern Recognition*, pages 2818–2827, 2020. 1, 6
- [39] Karen Simonyan and Andrew Zisserman. Very deep convolutional networks for large-scale image recognition. *arXiv preprint arXiv:1409.1556*, 2014. 6
- [40] Shupeng Su, Chao Zhang, Kai Han, and Yonghong Tian. Greedy hash: Towards fast optimization for accurate hash coding in cnn. *Advances in Neural Information Processing Systems*, 31, 2018. 6, 7
- [41] Jinpeng Wang, Ziyun Zeng, Bin Chen, Tao Dai, and Shu-Tao Xia. Contrastive quantization with code memory for unsupervised image retrieval. In *Proceedings of the AAAI Conference on Artificial Intelligence*, 2022. 1, 2, 3, 4, 5, 6, 7
- [42] Chen Wei, Huiyu Wang, Wei Shen, and Alan Yuille. Co2: Consistent contrast for unsupervised visual representation learning. In *International Conference on Learning Representations*, 2021. 3, 5, 8
- [43] Yair Weiss, Antonio Torralba, and Rob Fergus. Spectral hashing. *Advances in Neural Information Processing Systems*, 21, 2008. 2, 6, 7
- [44] Guile Wu, Xiatian Zhu, and Shaogang Gong. Tracklet self-supervised learning for unsupervised person re-identification. In *Proceedings of the AAAI Conference on Artificial Intelligence*, volume 34, pages 12362–12369, 2020. 2, 4
- [45] Zhirong Wu, Yuanjun Xiong, Stella X Yu, and Dahua Lin. Unsupervised feature learning via non-parametric instance discrimination. In *Proceedings of the IEEE Conference on Computer Vision and Pattern Recognition*, pages 3733–3742, 2018. 3
- [46] Erkun Yang, Cheng Deng, Tongliang Liu, Wei Liu, and Dacheng Tao. Semantic structure-based unsupervised deep hashing. In *Proceedings of the 27th International Joint Conference on Artificial Intelligence*, pages 1064–1070, 2018. 6, 7
- [47] Erkun Yang, Tongliang Liu, Cheng Deng, Wei Liu, and Dacheng Tao. Distillhash: Unsupervised deep hashing by distilling data pairs. In *Proceedings of the IEEE/CVF Conference on Computer Vision and Pattern Recognition*, pages 2946–2955, 2019. 1, 2
- [48] Qize Yang, Hong-Xing Yu, Ancong Wu, and Wei-Shi Zheng. Patch-based discriminative feature learning for unsupervised person re-identification. In *Proceedings of the IEEE/CVF Conference on Computer Vision and Pattern Recognition*, pages 3633–3642, 2019. 4
- [49] Tan Yu, Jingjing Meng, Chen Fang, Hailin Jin, and Junsong Yuan. Product quantization network for fast visual search. *International Journal of Computer Vision*, 128(8):2325–2343, 2020. 1, 2, 3, 4
- [50] Li Yuan, Tao Wang, Xiaopeng Zhang, Francis EH Tay, Zequn Jie, Wei Liu, and Jiashi Feng. Central similarity quantization for efficient image and video retrieval. In *Proceedings of the IEEE/CVF Conference on Computer Vision and Pattern Recognition*, pages 3083–3092, 2020. 1, 2
- [51] Maciej Zieba, Piotr Semberceki, Tarek El-Gaaly, and Tomasz Trzcinski. Bigan: Learning compact binary descriptors with a regularized gan. *Advances in Neural Information Processing Systems*, 31, 2018. 6